

Telecommunication Systems: Final Project

Analysis of the Downlink System for Low Earth Orbit CubeSats

Balossi Claudia, Corradetti Mario, Donato Giuseppe

Abstract

The purpose of this report is to illustrate the sizing of a space-Earth link capable of serving a 1U CubeSat. Typical dimensions proper of the academic research have been considered for the latter. The sizing of this downlink system has been carried out in accordance with the typical data volume produced by a CubeSat for telemetry. The frequency range considered is S-band. For the ground segment, ground stations that already exist and are part of the ESA network have been considered.

1 Introduction

One compelling area of current space research is the design of miniaturized satellites, known as CubeSats, which are enticing because of their numerous applications and low design-and-deployment cost. Thanks to the low cost, CubeSats represent the only chance for many universities to secure access to space. Miniaturization of the TTMTTC and ADCS subsystems has also allowed for increasingly robust satellites while still maintaining the small size. The analysis carried out in this report aims at describing a possible solution able to meet the requirements for a communication system for 1U cubesat ($10 \times 10 \times 10$ cm), taking in account the atmospheric effects as well as other losses.



Figure 1: 1U CubeSat

The average data volume considered is typical for telemetry, i.e., 1 Mbps, with maximum peaks of 105 Mbps. Considering also the properties of the ground stations taken into account,

a S-band carrier frequency, that is available for space science services[2], has been selected. The latter choice, besides being consistent with the ground segment, also respects the regulations and in addition respects the requirements imposed by the small size of the satellite and the proximity of the orbit, which will be illustrated below, to the Earth. The selection of the antenna to be mounted on the satellite was driven to meet all requirements imposed by the carrier frequency and class of the satellite. In particular, the choice fell on S-Band Patch Antenna RHCP for HISPCO[14], that is a planar, passive antenna characterized by small dimensions (50 mm x 50 mm x 3.2 mm) and low input power (up to 10 W). With RHCP, the antenna provides a robust solution regarding the steering accuracy to the ground station antenna. With the basic design TRL 9 has been achieved with various successful LEO missions.

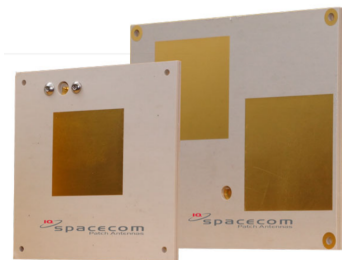


Figure 2: S-Band Patch Antenna RHCP for HISPCO

2 Atmospheric Propagation

In the design of Earth-space links for communication systems, several effects must be considered. Therefore, for the proper planning of Earth-space systems, it is necessary to have appropriate propagation data and prediction techniques capable of estimate the atmospheric attenuation. The overall attenuation represent the combined effect of both the non-ionized atmosphere (gas, cloud, rain and scintillation) and the ionosphere. These contributions are related to the value of p , which represent the probability that a given attenuation level is exceeded. A threshold value of $p=1\%$ has been selected for the sizing of the communication system. In addition, since the inclination of the selected orbit is non-zero, the variation of the elevation angle must be taken into account. Consequently, a minimum of 5 degrees of elevation was imposed so that a link could be established between the satellite and the ground station. All the attenuations have been computed by considering a frequency of 2228 MHz.

2.1 Gaseous Attenuation

In order to estimate the attenuation of atmospheric gases along slant path, the approximate method valid in the frequency range 1-350 Hz presented in ITU-R P.676-12-Annex 2 has been followed.

The first absorption's peak of oxygen and water vapour is located around 60 GHz and 22 GHz respectively, as shown in Fig. 3. Since the S-band frequency interval is well below the peaks, the proposed method can grant an accurate estimation.

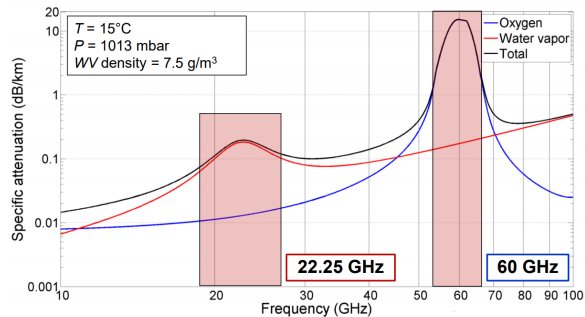


Figure 3: Specific attenuation from oxygen and water vapour, as function of frequency

The specific attenuation γ due to oxygen

(o) and water vapour (w) can be accurately evaluated at any location using the individual spectral lines from each gas, considering small additional factors for the non-resonant Debye spectrum of oxygen below 10 GHz, pressure-induced nitrogen attenuation above 100 GHz and a wet continuum to account for the excess water vapour-absorption found experimentally. This model is applicable to frequencies up to 1000GHz, and γ can be predicted as

$$\gamma_j = 0.1820 \cdot f \cdot N_j, \quad \text{where } j = o, w$$

where $N_o(f)$ and $N_w(f)$ are the imaginary parts of the frequency-dependent complex refractivities:

$$N_o''(f) = \sum_{i(\text{Oxygen})} S_i F_i + N_D''(f) \quad (1)$$

$$N_w''(f) = \sum_{i(\text{WaterVapour})} S_i F_i \quad (2)$$

S_i is the strength of the i -th oxygen or water vapour line, F_i is line shape factor (data have been taken from [7]).

$N_D''(f)$ is the dry continuum due to pressure-induced nitrogen absorption and the Debye spectrum and as well as S_i is a function of f , T , dry air pressure and water vapour partial pressure. The values of dry pressure, p , temperature, T , and water vapour density, ρ , are computed at the surface of the Earth, in correspondence of the location of the ground station. If the local data are not available, the mean annual global reference atmosphere given in Recommendation ITU-R P.835 [8] can be used for an estimation.

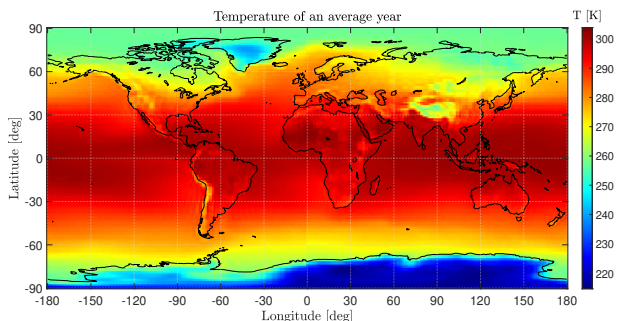


Figure 4: Mean annual temperature distribution at Earth surface

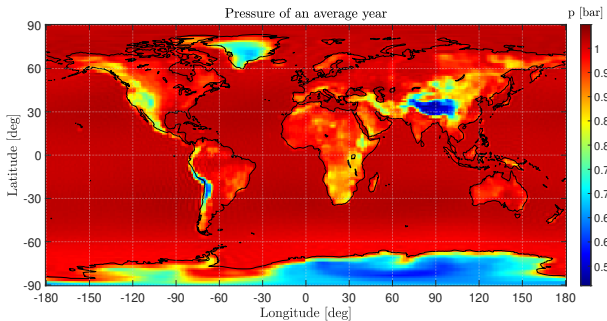


Figure 5: Mean annual pressure distribution at Earth surface

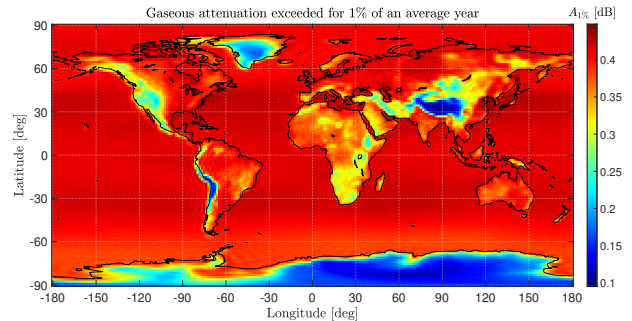


Figure 7: Total gaseous attenuation exceeded for 1% of an average year

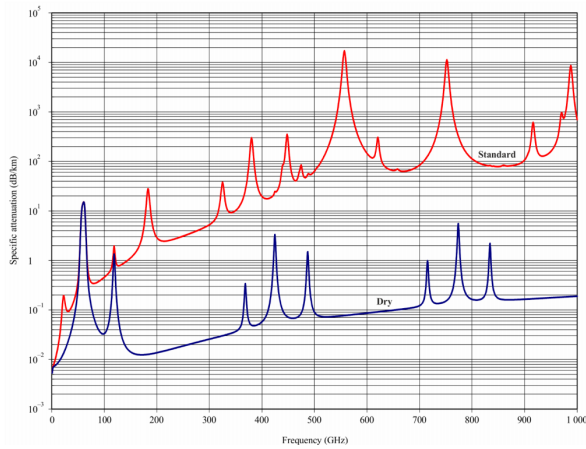


Figure 6: Specific attenuation due to atmospheric gases, calculated at 1 GHz intervals, including line centres

The total gaseous attenuation for slant paths through Earth's atmosphere can be estimated through the concept of equivalent heights, by which the specific attenuation is multiplied to obtain the corresponding zenith attenuation. The oxygen and water vapour specific attenuations are calculated at the pressure, temperature, and water vapour density at the Earth station's altitude , assuming an exponential decay in atmospheric specific attenuation versus altitude.

For an elevation angle $5^\circ < \theta < 90^\circ$, the path attenuation can be modeled as

$$A = \frac{A_o + A_w}{\sin \theta} \quad (3)$$

where $A_o = h_o \gamma_o$ and $A_w = h_w \gamma_w$ are the zenith attenuation of oxygen and water vapour respectively.

2.2 Rain Attenuation

The estimation of the long-term statistics of the slant-path rain attenuation at a given location has been carried out following the procedure presented in ITU-R P.618-13 [5], which is valid for frequencies up to 55 GHz.

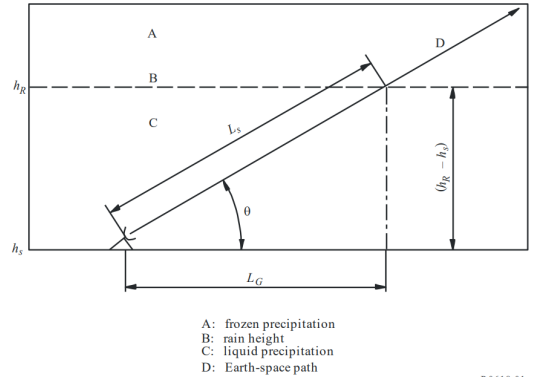


Figure 8: Schematic presentation of an Earth-space path giving the parameters to be input into the attenuation prediction process

The first step is to determine the rain height, as specified in Recommendation ITU-R P.839 [10]. The mean annual rain height above mean sea level, h_R , may be obtained from the 0° isotherm as:

$$h_R = h_0 + 0.36 \text{ km} \quad (4)$$

The value of the 0° isotherm, h_0 , is tabulated as function of latitude and longitude, as shown in the digital map Fig. 9, provided with the recommendation.

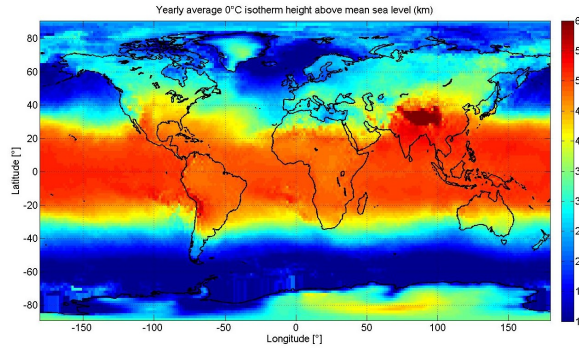


Figure 9: 0 degree isotherm height(in km and above mean sea level) for Rec. ITU-R P.839-4

Then, considering $\theta \geq 5^\circ$, the slant-path length (L_S) below the rain height can be computed from the following trigonometric relation:

$$L_S = \frac{h_R - h_S}{\sin \theta} \quad (5)$$

with the geometry reported in Fig. 8.

At this point the horizontal projection L_G of the slant-path length is retrieved from:

$$L_G = L_S \cos \theta \quad (6)$$

An estimate of the rainfall rate, $R_{0.01}$, exceeded for 0.01 % of an average year can be obtained from the maps of rainfall rate given in Recommendation ITU-R P.837.

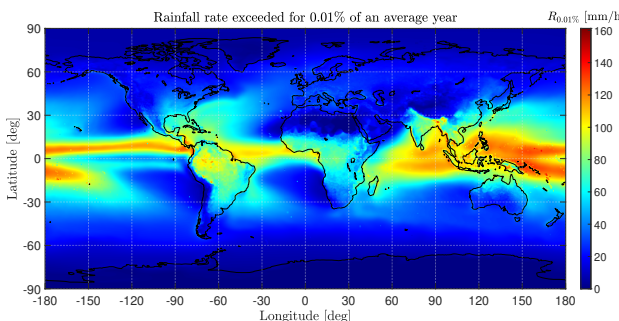


Figure 10: Rainfall rate exceeded for 0.01 % of an average year

The specific attenuation γ_R can be estimated using the rainfall rate and the frequency-dependent coefficients given in Recommendation ITU-R P.838 [9]:

$$\gamma_R = k(R_{0.01})^\alpha \quad (7)$$

Values for the coefficients k and α are determined as functions of frequency, in the range

from 1 to 1000 GHz, and are tabulated both for horizontal and vertical polarization. For linear and circular polarization the coefficients can be calculated through Eq. (8) and Eq. (9)

$$k = \frac{k_H + k_V + (k_H - k_V) \cos^2 \theta \cos 2\tau}{2} \quad (8)$$

$$\alpha = \frac{k_H \alpha_H + k_V \alpha_V + (k_H \alpha_H - k_V \alpha_V) \cos^2 \theta \cos 2\tau}{2k} \quad (9)$$

where θ is the path elevation angle and τ is the polarization tilt angle relative to the horizontal ($\tau = 45^\circ$ for circular polarization).

The predicted attenuation exceeded for 0.01 % of an average year at a given location is obtained from

$$A_{0.01} = \gamma_R L_E \quad (10)$$

where L_E is called the effective path length and depends on the previously computed parameters.

One may at this point extrapolate the value of attenuation exceeded for an arbitrary percentage of the year, in the range 0.001% to 5%. In our case we will consider $p = 1$ (i.e. 1%) and compute:

$$A_p = A_{0.01} \frac{p}{0.01}^{-[0.655 + 0.033 \ln(p) - 0.045 \ln(A_{0.01} - \beta(1-p) \sin \theta)]} \quad (11)$$

where

$$\beta = \begin{cases} 0 & \text{if } p \geq 1\% \text{ or } |\phi| \geq 36^\circ \\ -0.005(|\phi| - 36^\circ) & \text{if } p < 1\%, |\phi| < 36^\circ, \theta \geq 25^\circ \\ -0.005(|\phi| - 36^\circ) + 1.8 - 4.25 \sin \theta & \text{otherwise} \end{cases} \quad (12)$$

with ϕ latitude of the ground station, expressed in degrees. As a final result, in correspondence of $\theta = 5^\circ$, the rain attenuation map in Fig. 11 is obtained.

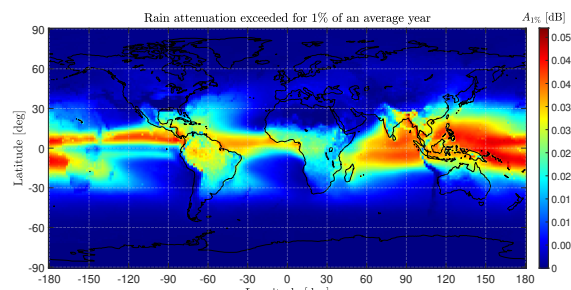


Figure 11: Rain attenuation exceeded for 1% of an average year

2.3 Cloud Attenuation

The model of attenuation due to the presence of small droplets in clouds and fog (ITU-R P.840.8 [11]) relies on Rayleigh's approximation and is valid for frequencies up to 200 GHz and droplet diameter < 0.01 cm.

The specific attenuation γ_c within the cloud (dB/km) can be expressed as

$$\gamma_c(f, T) = K_l(f, T)M \quad (13)$$

where f is the frequency (GHz), T is the cloud liquid water temperature (K), M is the liquid water density in clouds or fog (g/m^3) and K_l is the cloud liquid water specific attenuation coefficient ((dB/km)/(g/m^3)).

2.3.1 Cloud liquid water specific attenuation coefficient

The presented model is based on Rayleigh scattering, which uses a double-Debye model for the dielectric permittivity ε of water. Specifically

$$K_l(f, T) = \frac{0.819f}{\varepsilon''(1 + \eta'')} \quad (14)$$

where η'' is computed as

$$\eta'' = \frac{2 + \varepsilon'}{\varepsilon''} \quad (15)$$

ε' and ε'' denote the real and imaginary part of water's complex dielectric permittivity respectively and are computed from the model presented in [11]. Assuming an elevation angle $5^\circ < \theta < 90^\circ$, the slant path cloud attenuation is given by

$$A = \frac{L_{red}K_l}{\sin\theta} \quad (16)$$

where L_{red} is the total columnar content of liquid water reduced to a temperature of 273.15K and its values are available in the ITU-R P.840.8 documentation.

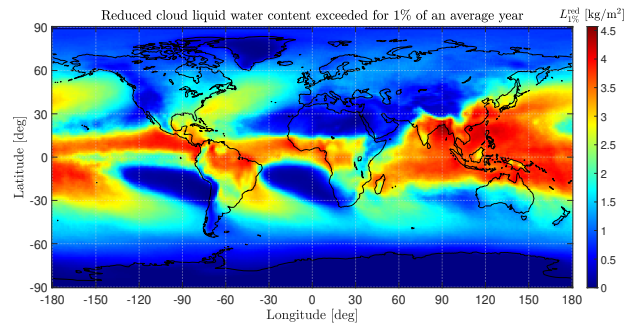


Figure 12: Reduced cloud liquid water content

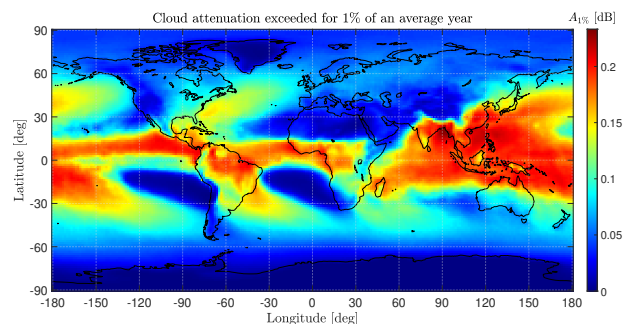


Figure 13: Cloud attenuation exceeded for 1% of an average year

2.4 Tropospheric Scintillation

Variations in refractive index caused by atmospheric turbulence can cause spatial and temporal fades and enhancements in signal strength. The physical process consists of alternating focusing and defocusing of a radio wave. Since the mechanism consists only of focussing and defocusing, not the absorption of energy, the net effect of tropospheric scintillation, when averaged over space and/or time, tends to zero. The tropospheric scintillation effect can be considered negligible below 4 GHz[6].

2.5 Ionospheric Attenuation

The ionosphere is a region of weakly ionised gas in the Earth's atmosphere lying between about 50 kilometers up to several thousand kilometers from Earth's surface. Solar radiation is responsible for this ionisation producing free electrons and ions. The ionosphere affects radio wave propagation in various ways such as refraction, absorption, Faraday rotation, group delay, time

dispersion or scintillations. Most of these effects are related to the Total Electron Content (TEC) in the propagation path, moreover, they are dispersive, as they depend on the signal frequency. The equatorial anomaly regions, located at around $\pm 15 \div 20$ degrees on either side of the magnetic equator, usually present the largest TEC values.

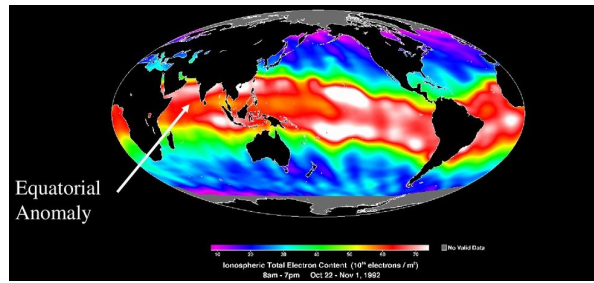


Figure 14: Ionospheric map

Mid-latitude regions daytime TEC values are usually less than half the value found in the equatorial anomaly region. Polar and auroral regions present moderate TEC values, but larger variability than in mid-latitudes due to the characteristics of the geomagnetic field. Ionospheric effects may be important, particularly at frequencies below 1 GHz, while these effects may be negligible at frequencies higher than about 12 GHz [5].

One of the most severe disruptions along a trans-ionospheric propagation path for signals below 3 GHz is caused by ionospheric scintil-

lation. Ionospheric scintillation effects may be observed occasionally up to 10 GHz. Scintillations are created by fluctuations of the refractive index, which are caused by inhomogeneities in the medium. Geographically, there are two intense zones of scintillation, one at high latitudes and the other centred within ± 20 degrees of the magnetic equator. Severe scintillation has been observed up to 10 GHz frequencies in these two sectors, while in the middle latitudes scintillation occurs exceptionally, such as during geomagnetic storms. Therefore, in order to be able to discard the ionosphere effects on the communication system, only middle latitude ground stations has been considered.

2.6 Total Atmospheric Attenuation

As already illustrated in the introduction of this chapter, the most critical condition for the sizing of the communication system turns out to be the corresponding attenuation level with an elevation angle of 5 degrees, that is exceeded of 1% of an average year. The overall atmospheric attenuation [5] can be computed with the formula:

$$A_{tot}(p) = A_{gas}(p) + \sqrt{[A_{rain}(p) + A_{cloud}(p)]^2 + A_{scint}(p)^2} \quad (17)$$

The figure Fig. 15 shows the map of atmospheric attenuation. In this map it is possible to find confirmation of the fact that mid latitudes are favorable compared to equatorial ones.

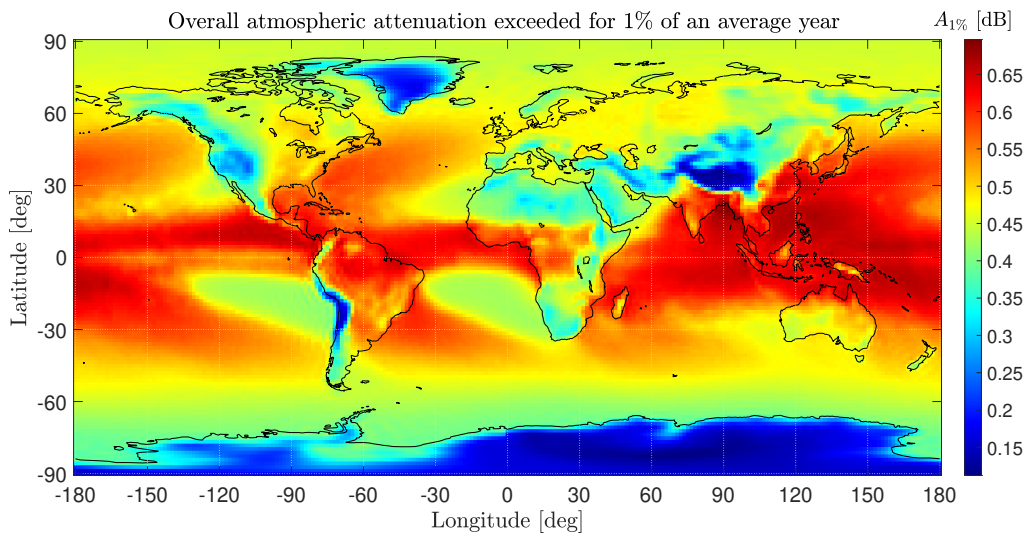


Figure 15: Overall attenuation

3 Downlink Budget

3.1 Orbit Definition

The largest number of missions making use of CubeSat are concentrated in LEO orbit. Consequently, the orbit selected for this analysis is also part of this orbital zone. The selected orbit is characterized by a very low eccentricity while the inclination is high enough to take advantage of ground stations located in the mid latitudes. The orbital parameter are reported in Table 1: the satellite performs 14 revolutions over the course of a day. Fig. 16 represents the groundtrack of the orbit for a single revolution.

Table 1: Orbital parameters

| a | e | i |
|---------|--------|----------|
| 7204 km | 0.0054 | 47.9875° |

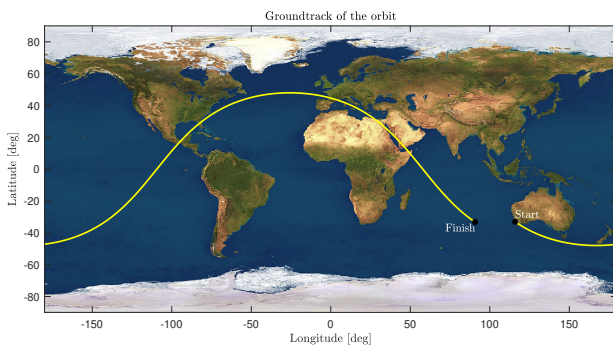


Figure 16: Orbit groundtrack

In the orbit propagation process, the orbital perturbation generated by the not perfectly spherical shape of the earth (J_2 perturbation) was taken into account, while the other perturbations (generally minor in the orbital zone taken into account) were not considered.

3.2 Ground Station Selection

As mentioned above, for the ground station selection process those belonging to the ESA network have been considered [1]. In addition, in order to respect the constraints due to atmospheric attenuation and orbit properties, only mid latitude ground stations have been considered. In particular, the ground stations on

which the analysis was carried out are:

- Villafranca ($40^\circ 26' 33''$, $-03^\circ 57' 5.7''$)
- St. Maria ($36^\circ 59' 50''$, $-25^\circ 08' 08.60''$)
- New Norcia ($-31^\circ 02' 54''$, $+116^\circ 11' 28''$)

All three selected ground stations support S-band. Fig. 17 shows the position of the three ground stations compared with the groundtrack of the orbit for a whole day.

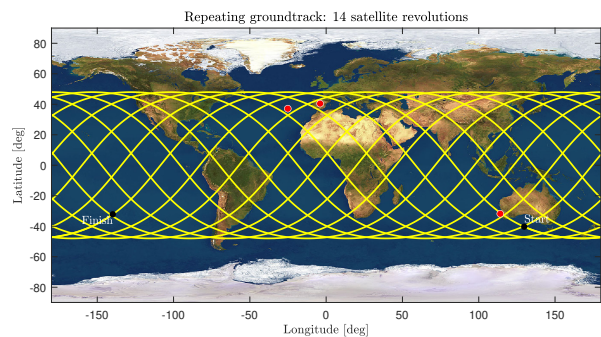


Figure 17: Repeating groundtrack for 14 satellite revolutions in one day

Finally, the parameter chosen to discriminate between the three ground stations and select the one that will be the space segment for the communication system is the visibility time. For the calculation of this parameter it is first necessary to calculate the satellite to station elevation angle.

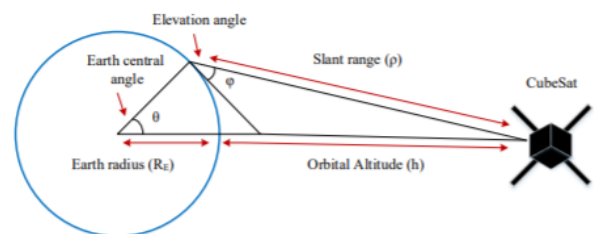


Figure 18: Coverage geometry for CubeSats.

The model used to calculate the elevation angle is based on the position vectors \underline{r}_{GS} and \underline{r}_{SC} of ground station and satellite respectively.

$$\underline{r}_{GS} = r_{GS} \begin{Bmatrix} \cos\phi_{GS} \cos\lambda_{GS} \\ \cos\phi_{GS} \sin\lambda_{GS} \\ \sin\phi_{GS} \end{Bmatrix} \quad (18)$$

$$\underline{r}_{SC} = r_{SC} \begin{Bmatrix} \cos\phi_{SC} \cos\lambda_{SC} \\ \cos\phi_{SC} \sin\lambda_{SC} \\ \sin\phi_{SC} \end{Bmatrix} \quad (19)$$

Having obtained the two vectors and defining $\Delta\mathbf{r} = \underline{r}_{SC} - \underline{r}_{GS}$ it is possible to proceed with the calculation of α :

$$\alpha = \arccos \left(\frac{\Delta\mathbf{r}}{\|\Delta\mathbf{r}\|} \cdot \frac{\underline{r}_{GS}}{\|\underline{r}_{GS}\|} \right) \quad (20)$$

Where α is the complementary angle of the elevation angle θ . Considering $\theta_{min}=5^\circ$ and discarding all the overflights shorter than 180s (non suitable to establish a stable link with the satellite) it is possible to compute the visibility time for each ground station. The results are reported in Table 2.

Table 2: Visibility time over one day (14 satellite revolutions)

| Ground station | Visibility time [min] |
|----------------|-----------------------|
| Villafranca | 16.13 |
| Santa Maria | 51.27 |
| New Norcia | 82.80 |

It is straightforward to note that the New Norcia station is the one that allows the most extensive visibility time. The reason can be found in Fig. 19 that highlights the visibility areas of the ground stations and the satellite ground-track. It can be seen that while the visibility area of New Norcia is almost completely inside the groundtrack, the visibility area of Villafranca (the ground station with the shortest visibility time) is almost half outside of it, being consequently less exploited to create links.

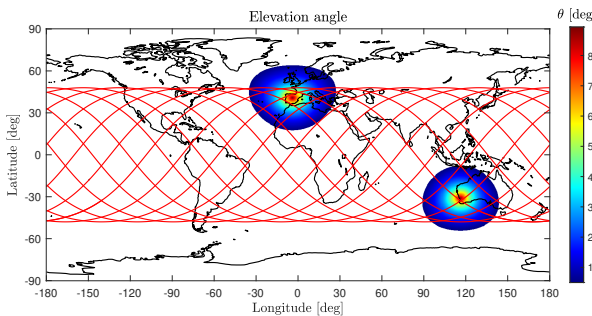


Figure 19: Surface area available for communication as function of satellite's elevation angle

Fig. 20 shows that the satellite can establish a link with the ground station seven times a day.

This means that, on average, the CubeSat can grant more than 10 minutes of connection.

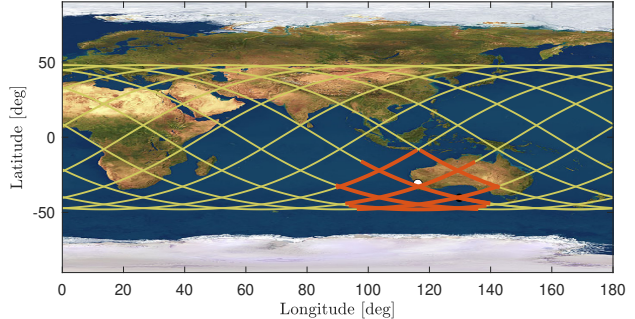


Figure 20: Satellite's passages over New Norcia ground station

The overall attenuation over New Norcia's ground station is depicted in Fig. 21, as function of the elevation angle.

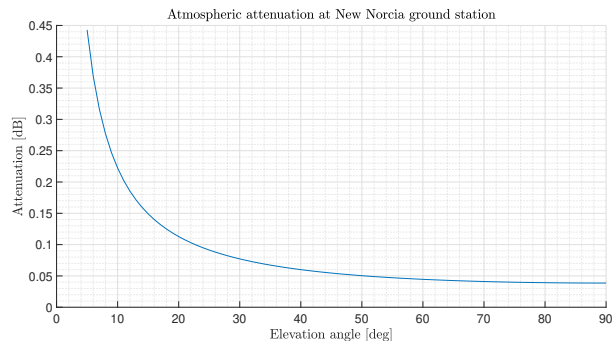


Figure 21: Overall attenuation at New Norcia ground station as function of elevation angle

A more accurate research about the presence of ionospheric scintillation over Australia has been carried out by studying the variation of the amplitude scintillation index, S4. This parameter, which is defined as the square-root of the normalised variance of signal intensity over a given interval of time, is a dimensionless number with a theoretical upper limit of 1. Strong scintillations are generally considered to occur when the S4 parameter is greater than 0.6 and are associated with strong scattering of the signal in the ionosphere. Moreover, an S4 level below 0.3 is unlikely to cause a significant impact on telecommunications.

Fig. 22 [16] and Fig. 23 [4] show that the intensity of S4 index over Western Australia is low enough to discard the ionospheric scintillation's effect in this preliminary model.

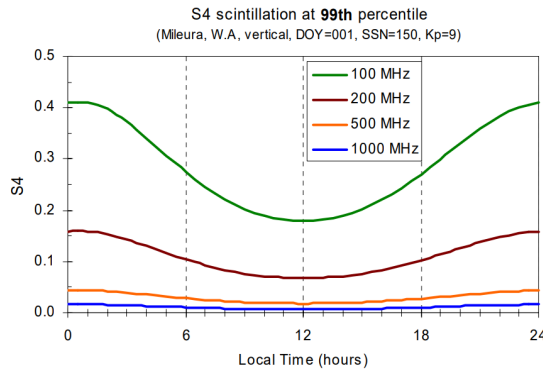


Figure 22: Extreme S4 values expected at Mileura Station, Western Australia

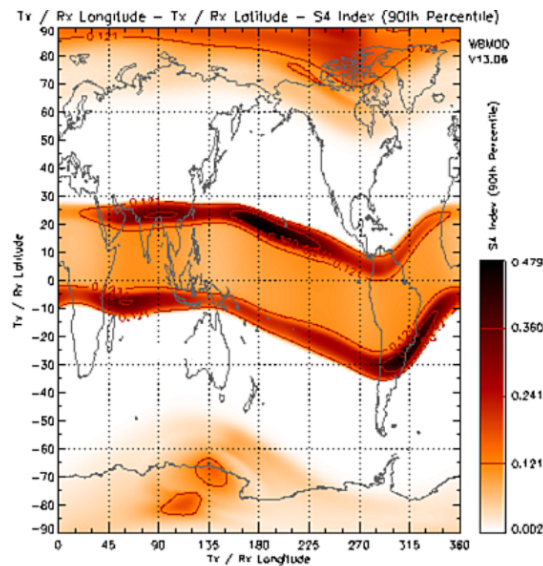


Figure 23: Scintillation index at 1.6 GHz assuming constant local time at all longitudes

3.2.1 Daily Throughput

The most common LEO CubeSat communication system design currently set the data volume at 3 Gb/day in S-band[12]. The HIPISCO transmitter datarate was considered for calculating the volume of downloadable data in a day. It is capable transmitting up to 1.6 Mbit/s using DQPSK (Differential Quadrature Phase Shift Keying) modulation, the forward error correction is a TURBO code with a rate of 0.489 [15]. Consequently, taking into account the visibility time calculated above, the connection between the CubeSat and the New Norcia station guarantees the possibility to download 5.27 Gb/day. Thus, the throughput goal of 3Gb/day is largely met.

3.3 Link Budget

A link budget is a set of parameters that define a communication link in terms of the power available for a reliable connection between the transmitter and receiver.

The Bit Error Rate (BER) is a useful parameter for measuring the quality of a digital communication link. This parameter is linked with the energy-per-bit to noise-power-density ratio (E_b/N_0) through a relationship strongly dependent on the coding scheme. As stated above the HIPISCO transmitter use the TURBO code, this provide error correction performance in low signal-to-noise ratio environments near the theoretical Shannon limit. Turbo coding provides a significantly improved error correction performance with respect to BPSK modulation, for short block is 5 dB better than BPSK[13]. The BER performance of a BPSK scheme has been obtain by means of `bertool`, which is part of Matlab Communication Toolbox, and is shown in Fig. 24.

As a result, imposing the threshold BER at 10^{-8} requires a $\left[\frac{E_b}{N_0}\right]_{min} = 7 \text{ dB}$.

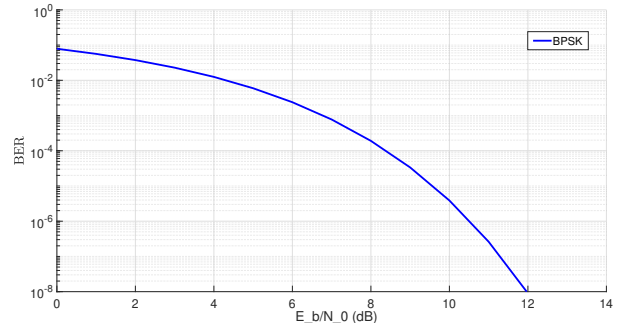


Figure 24: Calculated BER of BPSK Encoding

The energy-per-bit to noise spectral density at the ground station can be expressed as:

$$\frac{E_b}{N_0} = \frac{P_{tx} G_{tx} G_{rx}/T L}{k_B R_d} \quad (21)$$

Where P_{tx} is the transmitted power, G_{tx} and G_{rx} are the transmitter and receiver antenna gains, T is the system temperature noise, R_d is the target data rate, k_B is the Boltzmann constant, and L is the overall loss. The parameter used to compute the link budget are summarized in Table 3.

Table 3: Parameter of the link budget calculation

| | |
|---------------------------|-------------------------------|
| Transmitted Power | $P_{tx} = 27 \text{ dBm}$ |
| Transmitter Gain | $G_{tx} = 6 \text{ dBi}$ |
| Gain-to-noise temperature | $G_{rx}/T = 40 \text{ dB/K}$ |
| Pointing accuracy | $P_{acc,rx} = 5 \text{ mdeg}$ |
| Data rate | $R_b = 1.06 \text{ Mbps}$ |

The overall loss is given by:

$$L = L_{path} + L_{atm} + L_{pol} + L_{aml} + L_{add} \quad (22)$$

These losses represent, respectively: free-space path loss, atmospheric loss, polarization loss, antenna misalignment loss and additional losses due to transmitter/receiver chain .

- The free space loss is given by:

$$L_{path} = \left(\frac{\lambda}{4\pi d} \right)^2 \quad (23)$$

where d is the distance between the ground station and the satellite and λ is the wavelength of the signal. It is clear that the path loss is lower at the 90-degree elevation angle due to the shorter distance. It follows that the maximum distance is at the minimum elevation angle, i.e. at 5 degrees.

$$d = \sqrt{(R_E + r_{SC})^2 - R_E^2 \cos^2(\theta)} - R_E \sin(\theta) \quad (24)$$

with the geometry shown in Fig. 25.

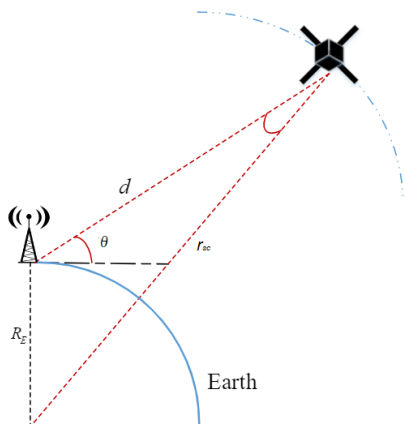


Figure 25: Schematic description of a LEO CubeSat trajectory

- The atmospheric loss L_{atm} has been computed in section 2, the exact value is the maximum of the graph in Fig. 21.
- Polarization loss, L_{pol} , occurs when a receiver is not matched to the polarization of an incident electromagnetic field. In this analysis, a value of 1 dB has been assumed.
- The misalignment losses are linked to the antenna pointing accuracy. For the receiving antenna at New Norcia ground station, the value has been computed as

$$L_{aml,rx} = -12 \left(\frac{D_{rx} P_{acc,rx}}{70\lambda} \right)^2 \quad (25)$$

- For what concerns the pointing loss of the transmitter, a value of 0.1 dB has been assumed [3].

All the resulting losses are summarized in Table 4.

Table 4: Parameter of the link budget calculation

| Loss | Absolute value |
|------------------------------------|----------------|
| Free-space path, L_{path} | 168.35 dB |
| Atmospheric loss, L_a | 0.45 dB |
| Polarization loss, L_{pol} | 1 dB |
| TX misalignment loss, $L_{aml,tx}$ | 0.1 dB |
| RX misalignment loss, $L_{aml,rx}$ | 0.004 dB |
| Additional loss, L_{add} | 5 dB |

To complete the link budget analysis, simply enter the values obtained into Eq. (21), obtaining a value of E_b/N_0 equal to 36.44 dB, which ensures a link margin of

$$\frac{E_b}{N_0} - \left[\frac{E_b}{N_0} \right]_{min} = 29.44 \text{ dB} \quad (26)$$

4 Conclusions

The analysis conducted in this report made it possible to verify the feasibility of a space-Earth link, capable of serving a LEO 1U CubeSat, using the S-band. Exploiting the visibility time as selection parameter, the station chosen as ground segment is the ESA New Norcia station, which is also characterized by low levels of atmospheric attenuation. Regarding the space

segment, a state-of-the-art antenna characterized by a high TRL was identified. The numerical analysis conducted had positive results with wide margins for both the daily data volume and the link budget. This report can be seen as a starting point for a more in-depth analysis, in which the limitations of the presented models, in particular the strong assumptions about ionospheric attenuation and orbit perturbations, are taken into account.

References

- [1] *Estrack ground stations*. URL: https://www.esa.int/Enabling_Support/Operations/ESA_Ground_Stations/Estrack_ground_stations.
- [2] Electronic Communications Committee (ECC) within the European Conference of Postal and Telecommunications Administrations (CEPT). “The European Table of Frequency Allocations and Applications in the frequency range 8.3 kHz to 3000 GHz (ECA Table)”. In: (2020), pp. 114–116.
- [3] *High Data Rate S-Band Transmitter*. Tech. rep. ISISPACE Group, 2021.
- [4] *Ionospheric scintillations*. URL: <https://www.sws.bom.gov.au/Satellite/6/3#impact>.
- [5] *ITU-R P.618 : Propagation data and prediction methods required for the design of Earth-space telecommunication systems*. URL: <https://www.itu.int/rec/R-REC-P.618-13-201712-I/en>.
- [6] *ITU-R P.619 : Propagation data required for the evaluation of interference between stations in space and those on the surface of the Earth*. URL: <https://www.itu.int/rec/R-REC-P.619/en>.
- [7] *ITU-R P.676 : Attenuation by atmospheric gases and related effects*. URL: <https://www.itu.int/rec/R-REC-P.676/en>.
- [8] *ITU-R P.835 : Reference Standard Atmospheres*. URL: <https://www.itu.int/rec/R-REC-P.835/en>.
- [9] *ITU-R P.838 : Specific attenuation model for rain for use in prediction methods*. URL: <https://www.itu.int/rec/R-REC-P.838/en>.
- [10] *ITU-R P.839 : Rain height model for prediction methods*. URL: <https://www.itu.int/rec/R-REC-P.839/en>.
- [11] *ITU-R P.840 : Attenuation due to clouds and fog*. URL: <https://www.itu.int/rec/R-REC-P.840/en>.
- [12] David Pierce James Schier William Horne. “NASA Near Earth Network (NEN) and Space Network (SN) CubeSat Communications”. In: (2016).
- [13] Michael Joost. “Turbo Codes”. In: () .
- [14] *S-Band Patch Antenna RHCP for HISPCO*. URL: <https://cubesatshop.com/product/s-band-patch-antenna-rhcp-hispc/>.
- [15] *S-Band Transmitter for Pico and Nanosatellites*. URL: <https://cubesatshop.com/product/highly-integrated-s-band-transmitter-for-pico-and-nano-satellite/>.
- [16] *The Australian Ionosphere , Input for the Australian SKA Proposal*. Tech. rep. SKA, 2005.